The existing stress measurement of the PC bridges by slit stress relief techniques using the optical full-field measurement method

Kenichi HIDA[1], Yukihiro ITO[2], Katsuya MITA[2],
Akira DEMIZU[3], Takuji OKAMOTO[4], Masaki YONEMOTO[4]

[1]K&T Consultant Co. Ltd; Tokyo, Japan,
Phone: +81-4-7141-0115, Fax: +81-4-7141-0116; e-mail: k-hida@kt-c.co.jp
[2]Saga University; Saga, Japan, e-mail: itoy@cc.saga-u.ac.jp, mita@cc.saga-u.ac.jp
[3]Nagasaki University; Nagasaki, Japan, e-mail: demizu@nagasaki-u.ac.jp
[4]Keisoku Research Consultant Co. Ltd; Hiroshima, Japan,
e-mail: okamoto@krcnet.co.jp,yonemoto@krcnet.co.jp

Abstract

Tendon of pre-stressed concrete bridge corrodes for damage from chloride attack, and pre-stress decreases. And a bridge falls by corrosion of PC-tendon. It is necessary to grasp the stress which acts on concrete of PC bridges.Therefore authors have developed the existing stress measurement method by slit stress relief techniques using the optical full-field measurement method.This report introduces a measurement method of pre-stress by the existing stress measurement method by slit stress relief techniques using the optical full-field measurement method.The following measured case of pre-stress of PC bridges will be reported.

1) Cause investigation in the central hinge bridge where I transformed abnormally
2) Confirmation of safety of the PC bridge damaged by chloride attack.
3) Decision of the strengthening amount of the PC bridge damaged by chloride attack

Keywords: optical full-field measurement method, slit stress relief technique, existing stress measurement

1. Introduction

Concrete structures are believed to be durable permanent structures. However, in recent years, remarkable changes in condition have been observed in some concrete structures. These changes include cracks and corrosion of reinforcing steel due to deterioration caused by chloride attack, carbonation, alkali-aggregate reaction, etc.

In post-tensioned prestressed concrete (hereinafter, PC) girders, cases of severe cracking or bridge collapse as a result of corrosion and rupture of PC tendons occurred due to chloride attack or hydrogen embrittlement fracture at points where grout filling was incomplete have been reported. There have also been cases in which prestress was reduced by unexpected creep/shrinkage, and deflection exceeding the design value occurred. Since a decrease in the prestress of a PC structure has a large effect on its load bearing capacity and leads to reduced safety, an accurate grasp of existing stress is necessary for proper maintenance of PC structures. However, the amount of existing prestress is not controlled; only the tensioning force of the PC tendons in the initial stage is controlled. The current methods for measuring the existing stress of PC structures include an estimation method in which strain gauges are placed on 3 axes and core stress is relieved, and a slot stress method developed in France, among others. [1] Because techniques for PC structures have same problems and have not been applied practically very much, a technique that enables accurate estimation is demanded. In order to improve accuracy in comparison with the conventional existing stress measurement methods, in this research, the authors developed an existing stress measurement method for PC structures by the stress relief method which is an existing stress measurement method, and the digital image correlation method. This method has features of highly accurate, noncontact and full-field measurement.

2. Existing stress measurement by slit stress relief technique using optical full-field measurement method

2.1 Overview

If a slit is cut perpendicular to the direction of stress in a concrete member on which uniform compressive stress acts, liberating strain will be generated in the area surrounding the slit. The analytical model of this technique is shown in Fig. 1. Figure 2 shows the relationship between the liberating strain and the distance from the slit center when the slit cutting depth in the model is changed from 10 mm to 20 and 30 mm.

As a feature of the existing stress measurement method by the slit relief technique developed in this research (hereafter, slit stress relief technique), the optical full-field measurement method is used in order to improve accuracy in comparison with the conventional method when measuring the liberating strain caused by slit-cutting.

In the slit stress relief technique, the area around the slit is measured with a full-field strain measurement device before and after cutting the slit, and the distribution of liberating strain is obtained from the measured images by the digital image correlation method, which is one optical full-field measurement method.

By using the optical full-field measurement method, strain measurements can be performed with high accuracy extending to micro areas in the vicinity of the slit. The existing stress of the concrete member is calculated based on the measured liberating stress distribution by inverse analysis by FEM analysis.

2.2 Optical full-field measurement method

The specifications of the optical full-field strain measurement device are shown in Table 1, and the appearance of the device is shown in Fig. 3. A mechanism that enables highly accurate travel was realized by fixing the drive device for sub-scanning on a high-rigidity frame to improve travel accuracy in the sub-scanning direction, and adopting two moveable linear guide rails for the line sensor and using a stepping motor in a precision ball screw in this part. A linear encoder with resolution of 0.1 µm is used to control the movement distance in the sub-scanning direction. A jig is attached so that the device can be attached easily and firmly to the object of measurement.

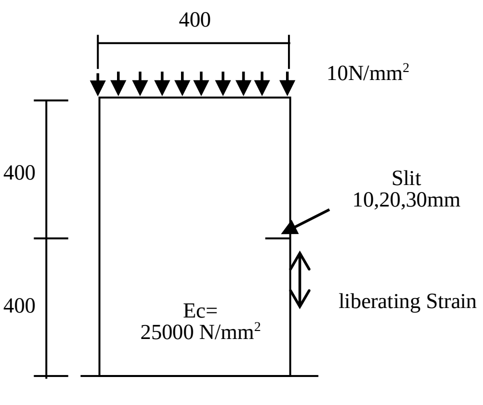

Figure 1. Analytical model

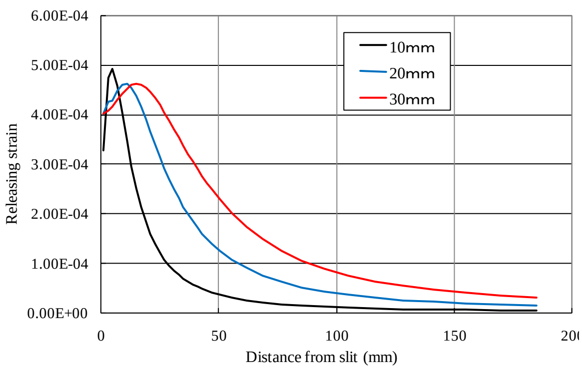

Figure 2. Distribution of liberating strain by slit-cutting

Table 1. Specifications

Sensor type	CIS
Greatest manuscript size	210×210mm
Optics resolution(main scanning × vice-scanning)	1200dpi×1200dpi (About0.021mm/pixel)
Source of light	LED
Power supply	DC15V
Electricity consumption	15W
Size (width × depth × height)	387mm×262mm ×90mm
Weight	About 8000g

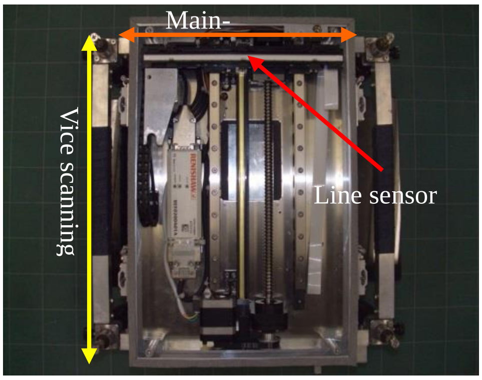

Figure 3. Optical full-field measurement device

2.3 Existing stress measurement by slit stress relief technique

The released strain distribution and change ratio distribution of the distance between the optical marks is obtained by applying the digital image correlation method to the photographed images. The digital image correlation method, as shown in Fig. 4, is an image analysis technique in which the amount of movement from the position before slit-cutting is obtained based on digital information of the pixel clusters in the initial image, by locating pixel clusters for the same digital information from the image after slit-cutting.

The change ratio distribution of the distance between the optical marks is obtained from the measured images by the digital image correlation method, and existing stress is then estimated by obtaining a change ratio distribution between optical marks that approximates the measured change ratio distribution by inverse analysis by FEM analysis.

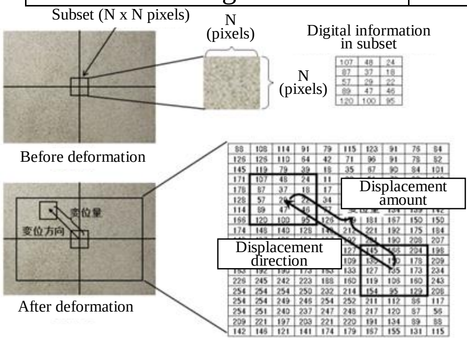

Figure 4. Digital image correlation method

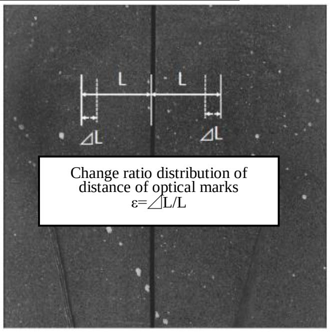

Figure 5. The object point distance rate of change

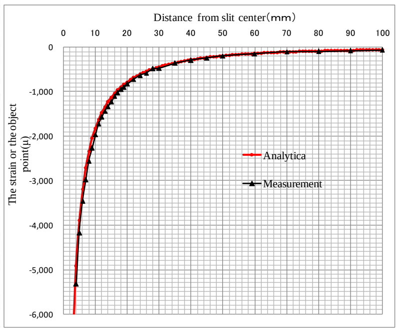

Figure 6. Example of the strain distribution of object point

The change ratio distribution between optical marks, as shown in Fig. 5, is the ratio of the change in distance between two points, assuming the slit is the center of that distance. Existing stress is estimated from the analysis values obtained by inverse analysis by FEM analysis which coincide with the measured values by using the analytical model shown in Fig. 7 and the mesh diagrams shown in Fig. 8. Figure 6 shows an example of the change ratio distribution of the optical marks of the analytical values and the measured values at the center of a span. Figure 9 shows the work procedure.

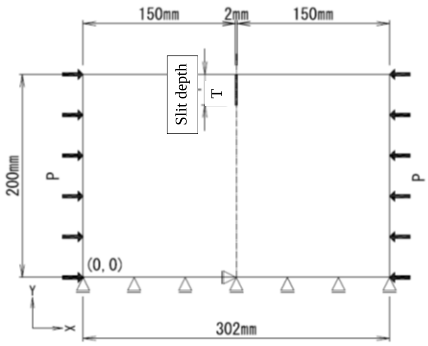

Figure 7. Analytical model

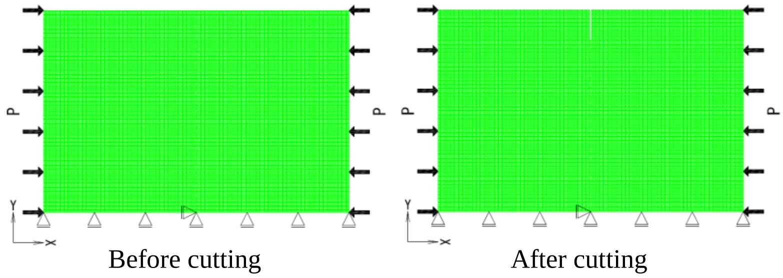

Figure 8. Mesh diagrams

1. Rebar probe Using a reinforcing bar probe, the PC tendon position is confirmed and the measurement position is decided.		4. Initial image The initial image is photographed with a flat scanner.	
2. Surface treatment The surface is smoothed to enable photography of focused images.		5. Slit-cutting slit-cutting is performed with a dedicated cutter.	
3. Surface condition before stress relief A random black and white pattern is attached.		6. Photography after stress relief The image after slit-cutting is photographed with the flat scanner.	

Figure 9. Work procedure

3. Cause investigation of abnormal deformation of central hinge bridge

3.1 Overview

This bridge is a 3-span hinge PC box girder rigid frame bridge which was constructed in a mountainous area in 1989. Abnormal deflection occurred in the central hinge part. The maximum deflection, as shown in Fig. 10, is approximately 140 mm. Focusing on inadequate prestress and creep deformation in the pier capital section, a study of stress (strain) in the central hinge bridge was carried out to determine the cause of this abnormal deformation. [2] In this stress investigation, the existing strain of the reinforcing steel was measured by the slit stress relief technique and the rebar cutting method. The investigation positions are shown in Fig. 11. Cross sections of pier capitals P1 and P2 were taken.

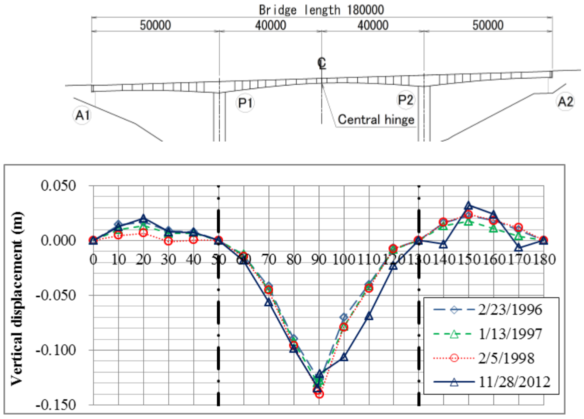

Figure 10. Transition of deflection

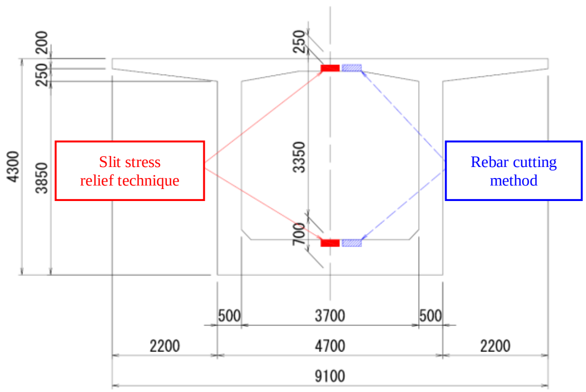

Figure 11. Investigation positions

Table 2. Measurement results

Measurement position		Slit stress relief technique		Rebar cutting method
		Existing stress σ_C	Strain of concrete ε_C	Strain of rebar ε_r
P1 pier capital	Upper slab	3.89±0.38 N/mm^2	177×10^{-6}	1334×10^{-6}
	Lower slab	5.10±0.59 N/mm^2	232×10^{-6}	1378×10^{-6}
P2 pier capital	Upper slab	1.73±0.44 N/mm^2	79×10^{-6}	916×10^{-6}
	Lower slab	6.33±0.63 N/mm^2	288×10^{-6}	1328×10^{-6}

3.2 Measurement results

The measurement results are shown in Table 2. From the results of sample core tests, the elastic modulus of the concrete was assumed to be E_C=22 kN/mm^2. Creep/Shrinkage and elastic strain, which were the existing strain at those positions, had occurred in the reinforcing steel arranged in the PC bridge. That is, the liberating strain which was measured by the rebar cutting method included elastic strain and creep/shrinkage. Therefore, if the existing stress of the concrete can be measured, creep/ shrinkage strain can be separated from the liberating strain obtained by the rebar cutting method by using Eq. (1).

$$\varepsilon_r=\varepsilon_l+\varepsilon_{\varphi s}=\sigma_c/E_C+\varepsilon_{\varphi s} \qquad (1)$$

where, ε_r: rebar strain, ε_l: elastic strain of rebar ($\varepsilon_l=\sigma_c/E_C$), $\varepsilon_{\varphi s}$: creep/shrinkage strain of concrete, σ_c: concrete stress (N/mm^2), E_c: elastic modulus of concrete (N/mm^2).

3.3 Estimation of cause of abnormal deflection of center hinge

Figure 12 shows the strain distribution diagram of the P1 pier capital for rebar strain (ε_r), which includes concrete strain (ε_c), i.e., a type of elastic strain, and drying shrinkage. ε_r and ε_c show substantially the same slopes. Assuming that drying shrinkage strain (ε_{sh}) and

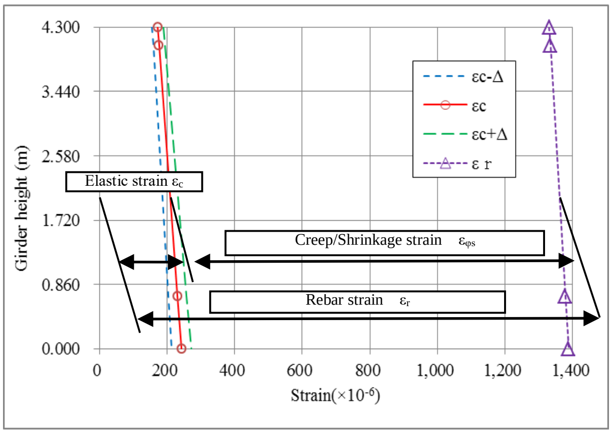

Figure 12. Strain distribution (measured) of P1 pier head

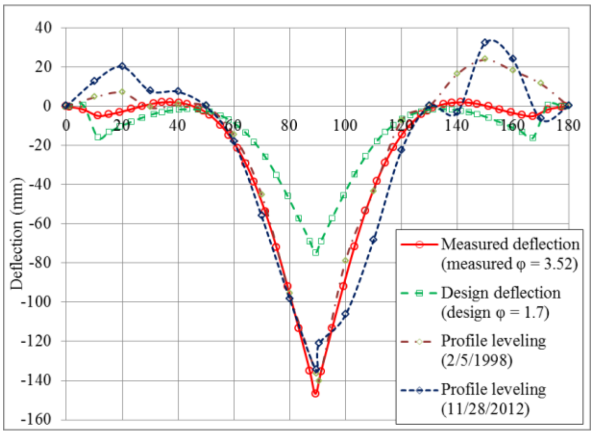

Figure 13. Deflection distribution by estimated creep coefficient

Table 3. Estimated creep coefficients and shrinkage

Measurement position	Girder height (m)	$\varepsilon_r\times10^{-6}$	$\varepsilon_c\times10^{-6}$	$\varepsilon_{\varphi s}\times10^{-6}$	n	$\varepsilon_{sh}\times10^{-6}$	φ
P1 pier capital	4.300	1330.7	172.7	1158.0	2.3	469.2	3.99
	4.050	1334.0	176.8	1157.2	2.3	462.3	3.93
	0.700	1378.0	231.8	1146.2	1.9	385.9	3.28
	0.000	1387.2	243.3	1143.9	1.9	372.8	3.17
	Average					422.6	3.59
P2 pier capital	4.300	885.3	63.0	822.2	2.7	535.4	4.55
	4.050	916.0	78.6	837.4	2.5	501.9	4.27
	0.700	1328.0	287.7	1040.3	1.5	301.9	2.57
	0.000	1414.1	331.4	1082.7	1.4	283.6	2.41
	Average					405.7	3.45

* Average creep coefficient of P1 and P2 pier capitals: φ=3.52

creep strain (ε_φ) are proportional to the design shrinkage strain and the design creep coefficient, the shrinkage and creep coefficient of the P1 and P2 pier capital parts can be obtained by Eq. (2).

$$\varepsilon_{\varphi s} = \varepsilon_{sh} + \varepsilon_\varphi = n \cdot (\varepsilon_{sh0} + \varepsilon_c \cdot \varphi_0) \qquad (2)$$
$$\varepsilon_{sh} = n \cdot \varepsilon_{sh0},\ \varepsilon_\varphi = n \cdot \varepsilon_c \cdot \varphi_0,\ \varphi = n \cdot \varphi_0$$

where, ε_{sh}: shrinkage strain, ε_φ: creep strain, φ: estimated creep coefficient, ε_{sh0}: design shrinkage (200×10^{-6}), φ_0: design concrete creep coefficient (1.7).

Table 3 shows the estimated creep coefficients and shrinkage. As these values are approximately the same, they are considered to express the creep coefficient and drying shrinkage of the actual bridge. Figure 13 shows the calculated deflection values calculated using the average estimated creep coefficient (φ=3.52) and the results of longitudinal leveling. Because the calculated values of deflection using the estimated creep coefficients are in good agreement with the results of longitudinal leveling, it is thought that the main cause of the abnormal deflection in this bridge is creep deformation.

4. Confirmation of safety of PC bridge damaged by chloride attack

4.1 Overview

This bridge is a post-tensioned PCT girder bridge which passes over a sea area and had been in service for approximately 40 years since construction. The bridge, as shown in Fig. 14, had suffered progressive deterioration in the forms of loose and peeling scale and corrosion of the reinforcing steel, and a reduction of load bearing performance was feared as a result of progress of corrosion of the members due to chloride attack and corrosion of the PC tendons. Therefore, a stress investigation, etc. was carried out to confirm the load bearing capacity of the bridge. [3] In the stress investigation, generated strain was measured by the slit stress relief technique and a dynamic load test assuming the service load. The measurement positions are shown in Fig. 15.

4.2 Measurement results

Table 4 shows the results of measurements by the slit stress relief technique, and Table 5 shows the results of the dynamic load test. As the elastic modulus, the design elastic modules at the time of construction, E_c=35 kN/mm^2 was assumed. In the dynamic load test, a dump truck with a gross weight of 20 t and a 50 t class rafter crane with a gross weight of approximately 40 t were assumed as the load vehicles. One lane was closed to traffic, the load vehicles were stopped in the center of the span on the closed lane, and the vehicles were allowed to travel on the open land when no general vehicles were passing. Measurements were performed under the following three load vehicle patterns.

Pattern 1: Dump truck stops on closed lane, dump truck travels on open lane.
Pattern 2: Dump truck stops on closed lane, rafter crane travels on open lane.
Pattern 3: Rafter crane stops on closed lane, dump truck travels on open lane.

Figure 14. Deterioration of main girder

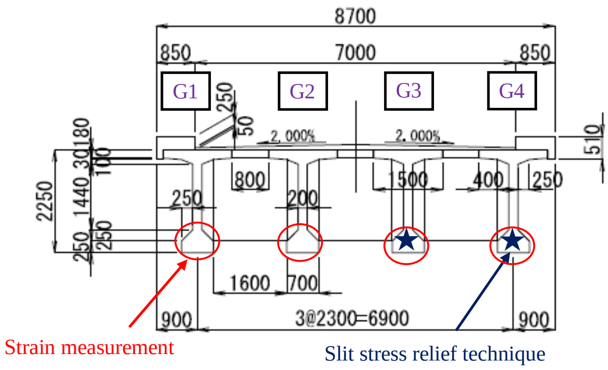

Figure 15. Measurement positions (span center)

Table 4. Results of measurement by slit stress relief technique

Measurement position	Existing stress (N/mm^2)		Error
G3	3.46 ± 0.15	3.31 - 3.61	4.3%
G4	3.21 ± 0.25	2.96 - 3.46	7.7%

Table 5. Results of dynamic load test

		G1	G2	G3	G4
Pattern 1	(A) Dump truck load	-0.2	-0.5	-0.8	-0.8
	(B) Dump truck load (traveling)	-1.1	-0.9	-0.6	-0.3
	(A)＋(B)	-1.3	-1.4	-1.4	-1.1
Pattern 2	(A) Dump truck load	-0.3	-0.5	-0.8	-0.9
	(B) Crane load (traveling)	-1.6	-1.4	-0.9	-0.5
	(A) + (B)	-1.9	-1.9	-1.7	-1.4
Pattern 3	(A) Crane load	-0.5	-0.9	-1.3	-1.3
	(B) Dump truck load (traveling)	-1.0	-0.9	-0.6	-0.4
	(A)＋(B)	-1.5	-1.8	-1.9	-1.7
Max. tensile stress	Dump truck single load	-1.1			
	Crane single load	-1.6			
	Dump tuck + dump truck parallel load	-1.4			
	Dump tuck + crane parallel load	-1.9			

Unit: N/mm^2 Compressive (+), tensile (-)

4.3 Evaluation of load bearing performance

In the PC girder of this bridge, from Table 4, the existing stress, which was stress on the resistance side, has become compressive stress of approximately 3.0 N/mm^2 or more. On the other hand, from Table 5, the maximum tensile stress due to single loading by a dump truck, which seems to have a high possibility of being the actual loading mode, is on the order of 1.0 N/mm^2. The maximum tensile stress due to single loading by a dump truck and parallel loading by dump trucks, which appear to have a small possibility, is about 1.5 N/mm^2, and the maximum tensile stress due to parallel loading by a dump truck and a rafter crane, which seems to have an extremely small possibility, is about 2.0 N/mm^2. Accordingly, the PC girder of this bridge is considered to be safe at the present point in time.

5. Design of Strengthening for PC bridge damaged by chloride attack

5.1 Overview

This structure is a pre-tensioned PCT girder comprising the superstructure of a rock shed which is in contact with the sea coast. It had been in service for approximately 30 years. In the structure, as shown in Fig. 16, deterioration in the forms of loose and peeling scale and corrosion of steel materials has progressed, and a reduction of load bearing performance was feared as a result progressive corrosion of the steel materials due to chloride attack and corrosion of the PC tendons. Therefore, an investigation by the slit stress relief technique was performed to confirm the loading bearing performance of the structure. The investigation positions were the six main girders on the lower side of the structure.

5.2 Measurement Results

The measurement results are shown in Table 6. As the elastic modulus of the concrete, the design elastic modulus at the time of construction, E_C=35 kN/mm^2 was assumed.

Figure 16. Damage of main girder

Table 6. Results of measurement by slit stress relief technique

Measurement position	Existing stress (N/mm^2)	Error (N/mm^2)	Standard deviation (%)
No. 14 Sea	2.27	1.67	71.3
No. 15 Mountain	-0.62	0.05	7.1
No. 16 Mountain	1.18	0.51	40.8
No. 20 Sea	0.95	0.64	63.1
No. 25 Mountain	0.11	0.04	35.5
No. 29 Sea	0.8	0.46	54.3

Existing stress : Compressive (+), tensile (-)

Table 7. Reduction of prestress

Measurement position	Existing stress (N/mm^2)	Prestress (N/mm^2)	Tensioning force (kN)	Reduction (%)
	σ_{cl}'	$\sigma_{cp}'=\sigma_{cl}'-\sigma_{dl}-\sigma_{sl}$	$P_t'=\sigma_{cp}'(1/A_c+y_{ep}/Z_l)$	Pt'/Pt
No 14 Sea	2.27	5.16	405.4	119.60%
No. 15 Mountain	-0.62	2.27	178.2	52.60%
No. 16 Mountain	1.18	4.07	319.7	94.30%
No. 20 Sea	0.95	3.84	301.6	89.00%
No. 25 Mountain	0.11	3.00	235.6	69.50%
No. 29 Sea	0.80	3.69	289.8	85.50%

Section area	Ac=	2.93E+05	(mm^2)
Section modulus	Zl=	-3.29E+07	(mm^3)
Steel eccentricity	y_{ep}=	-305.5	(mm)
Effective tensioning force	Pt=	$P_{t0}*\eta$= 338.9	(kN)

Average	85.10%
Standard deviation	20.80%
Lower limit	64.30%
Upper limit	105.90%

5.3 Evaluation of load bearing performance

The estimated results of the decrease of prestress are shown in Table 7. The amount of decrease of the prestress of the PC girders of this rock shed was 85.1% ±20.8% of the design prestress. Therefore, for the amount of prestress of the PC girders of the rock shed, the amount of strengthening was set assuming 60% of the design prestress, which was the lower limit of the estimated reduction of prestress.

5.4 Design of Strengthening

Bending strengthening of the PC girders of the PC rock shed, assuming 60% of the design prestress, was carried out by using 1 layer of high modulus carbon fiber sheet by the carbon fiber sheet adhesive method. In addition, 2 layers of middle modulus type carbon fiber sheet were used for shear strengthening. The cross section of the strengthening of the rock shed is shown in Fig. 17.

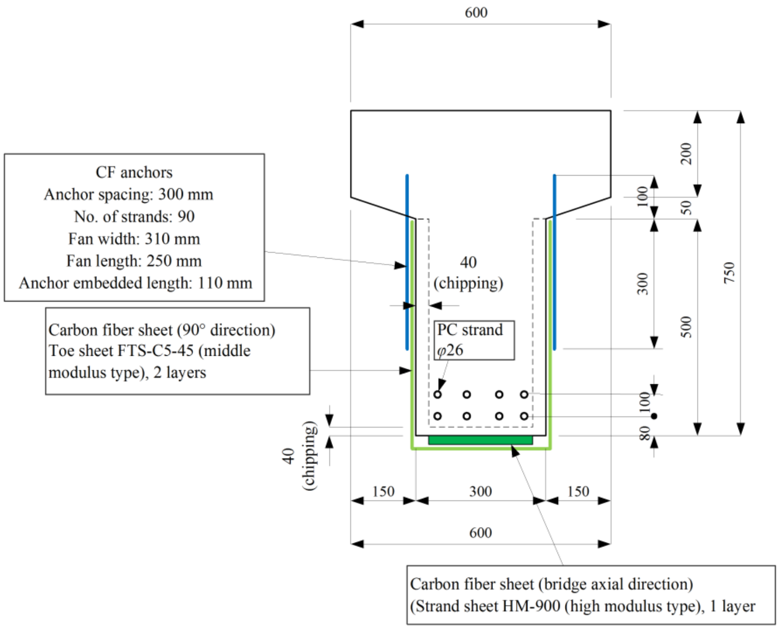

Figure 17. Sectional view of reinforcement

6. Conclusions

1) It is possible to separate creep/drying shrinkage strain from concrete stress (strain), which is a type of elastic stress, and estimate the creep coefficient of existing structures by using a combination of the slit stress relief technique and strain measurement of reinforcing steel by the rebar cutting method.

2) The load bearing capacity of existing PCT girder bridges, in which a reduction of prestress due to deterioration caused by chloride attack is an issue, can be evaluated by a comparative study of the resistance stress obtained by the slit stress relief technique, and the acting stress obtained by strain measurements in the dynamic load test supposing the service load.

3) The amount of reduction of prestress can be estimated from the results of the slit stress relief technique, and the proper load bearing performance can be evaluated. The proper amount of strengthening can then be set based on the amount of prestress (existing prestress) in the current condition.

References

1. Akira Demizu, Kenichi Hida, Yukihiro Ito, Masakazu Uchino, Takuji Okamoto, Hiroshi Matsuda: Measurement of existing stress of post-tensioned girders by optical technique and stress release method, Proceedings of the Annual Conference on Experimental Mechanics, Japanese Society for Experimental Mechanics, No. 10 GS5-5, pp281-286, 2010

2. Kenichi Hida, Yukihiro Ito, Mitsuaki Tsukihara, Haruyuki Koitabashi: "Report of investigation of central hinge bridge in which abnormal deformation occurred after approximately 30 years in service," Proceedings of the 22nd Symposium, pp345-348, 2013.10

3. Kenichi Hida, Yukihiro Ito, Akira Demizu, Masakazu Omachi: "Report on investigation of load bearing capacity of post-tensioned PCT girder bridge with damage by chloride attack," Proceedings of the 23rd Symposium, pp649-652, 2014.10